

# Numerical analysis of three-band models for CuO planes as candidates for a spontaneous T violating orbital current phase

Ronny Thomale and Martin Greiter

*Institut für Theorie der Kondensierten Materie, Universität Karlsruhe, D 76128 Karlsruhe*

(Dated: October 25, 2018)

Recently, we have numerically evaluated the current-current correlation function for the ground states of three-band models for the CuO planes of high- $T_c$  superconductors at hole doping  $x = 1/8$  using systems with 24 sites and periodic boundary conditions. In this article, the numerical analysis is explicated in detail and extended to a wider range of parameters. Our results show no evidence for the time-reversal symmetry violating current patterns recently proposed by Varma. If such current patterns exist, our results indicate that the energy associated with the loop currents must be smaller than 5 meV per link even if the on-site chemical potential on the oxygen sites, which is generally assumed to be of the order of 3.6 eV, is taken to zero, as advocated by Varma. We also vary the inter-atomic Coulomb repulsion scale and find only a weak dependence on this parameter. So while our studies do not rule out the existence of such current patterns, they do rule out that quantum critical fluctuations of these patterns are responsible for phenomena occurring at significantly higher energies such as the superconductivity or the anomalous properties observed in the strange metal phase provided the CuO superconductors are adequately described by any of the three-band models discussed.

PACS numbers: 74.20.Mn, 74.72-h, 74.20.-z

## I. INTRODUCTION

High- $T_c$  superconductivity (HTSC) has been one of the most active fields of research in condensed matter physics in the past two decades<sup>1,2</sup>. It has turned out to be an exceedingly difficult problem, with much of the effort invested just deepening the mysteries, but it has also led to a plethora of new developments extending far beyond the field. Many ideas, even though too general to qualify as complete theories of the cuprates, have inspired a vast amount of research in both high- $T_c$  and other areas. Most prominently among them are the notions of a resonating valence bond (RVB) state<sup>3</sup>, the gauge theories of antiferromagnetism<sup>4</sup>, and the notion of quantum criticality<sup>5</sup>. There have been, however, a few concise proposals which make falsifiable predictions. Intellectual masterpieces among them have been the theory of anyon superconductivity<sup>6</sup>, the proposal of kinetic energy savings through interlayer tunneling<sup>7</sup>, the SO(5) theory of a common order parameter for superconductivity and magnetism<sup>8</sup>, and a more recent proposal that the anomalous properties of the cuprates may be due to quantum critical fluctuations of current patterns formed spontaneously in the CuO planes<sup>9,10</sup>. In a recent Letter<sup>11</sup>, we investigated this proposal by finite cluster calculations. Here, we provide supplemental information and a more elaborate account of the approach.

This paper is organized as follows. In Section II, we briefly review Varma's proposal of spontaneous T violation in the CuO planes and discuss some assumptions made therein. In Section III, we introduce the three-band model Hamiltonian we investigate. In Section IV, we compute the current-current correlations of the ground state which we use to obtain information about the existence of orbital currents and the magnetic moment as-

sociated with them. We find that if an orbital current phase exists in the cuprates, the energy associated with the spontaneous currents will not be sufficiently high for the phase to account for the strange metal phenomenology in the cuprates. We derive an upper bound for the magnetic moment per unit cell from the upper bound we obtain for spontaneous currents, and find it smaller than the magnetic moment measured in a recent neutron scattering experiment<sup>12</sup>. The comparison shows, however, that even if the observed magnetic moments were due a current pattern as proposed by Varma<sup>9,10</sup>, the magnitude of these currents would be insufficient to determine the phase diagram. In search for an alternative explanation of the experiment, we investigate the spin-spin correlations of the ground state in Section V. In Section VI, the results for various three-band model parameters are presented. In particular, we vary the on-site chemical potential on the oxygens  $\epsilon_p$  from previously 3.6 to 1.8, 0.9, 0.4, and finally 0 eV. Furthermore, we vary the Coulomb interaction scale  $V_{pd}$  from 1.2 to 2.4 eV. The conclusion regarding the relevance of an orbital current pattern for the strange metal phase of CuO superconductors we reached previously remain intact. In Section VII, we discuss the the role of finite size effects in our numerical experiments, with particular emphasis on the net spin 1/2 of our finite size ground states. In Section VIII, we conclude that while we cannot rule out that the orbital current phase exists in the cuprates, we can infer that the energy associated with these fluctuations is not sufficiently high to account for the strange metal phase in the cuprates.

## II. HYPOTHESIS OF SPONTANEOUS T VIOLATION IN THE CUPRATES

The proposal of a spontaneous symmetry breaking through orbital currents is motivated by experiment. The normal state of the cuprates at optimal doping shows a behavior which can be classified as quantum critical, and has been rather adequately described by a phenomenological theory called marginal Fermi liquid<sup>13</sup>. The linear temperature dependence of the normal-state resistivity in optimally doped LSCO and YBCO<sup>14,15,16</sup>, which persists over several magnitudes of temperature, provides striking evidence in favor of this picture. The marginal Fermi liquid phenomenology led Varma to assume a quantum critical point (QCP) at a hole doping level of  $x_c \approx 0.19$ , an assumption consistent with a significant body of experimental data<sup>16,17,18,19,20</sup>. Critical fluctuations around this point are then held responsible for the anomalous properties of the strange metal phase, and provide the pairing force responsible for the superconducting phase which hides the QCP.

Interpreting the phase diagram in these terms, one is immediately led to ask what the phase to the left of the QCP, *i.e.*, for  $x < x_c$ , might be. The theory would require a spontaneously broken symmetry beyond the global U(1) symmetry broken through superconductivity. In addition, as the fluctuations are assumed to determine the phase diagram up to temperatures of several hundred Kelvin, the characteristic energy scale of the correlations associated with this symmetry violation must be at least of the same order of magnitude. No definitive evidence of such a broken symmetry has been found up to now, even though several possibilities have been suggested. These include stripes<sup>21</sup>, a  $d$ -density wave<sup>22</sup>, and a checkerboard charge density wave<sup>23</sup>.

The general consensus is that the low energy sector of the three-band Hubbard model proposed for the CuO planes<sup>24</sup> (see (1) below) reduces to a one-band  $t$ - $t'$ - $J$  model, with parameters  $t \approx 0.44$ ,  $t' \approx 0.06$ , and  $J \approx 0.128$  (energies throughout this article are in eV)<sup>25,26,27,28,29</sup>. However, two remarks are in order. First, the parameters are not exactly known, but can only be calculated approximately<sup>30</sup>. Second, for certain regimes of the phase diagram, CuO two-leg ladder studies have shown that the one-band and three-band description lead to qualitatively different results<sup>31,32</sup>.

For the undoped CuO planes, the formal valances are  $\text{Cu}^{2+}$  and  $\text{O}^{2-}$ . As the electron configuration of Cu atoms is  $[\text{Ar}] 3d^{10}4s^1$ , this implies one hole per unit cell, which will predominantly occupy the  $3d_{x^2-y^2}$  orbital. As the on-site potential  $\epsilon_p$  in the O  $2p_x$  and  $2p_y$  orbitals relative to the Cu  $3d_{x^2-y^2}$  orbital is generally assumed to be of the order of  $\epsilon_p = 3.6$  (with  $\epsilon_d = 0$ ), and hence smaller than the on-site Coulomb repulsion  $U_d \approx 10.5$  for a second hole in the  $3d_{x^2-y^2}$  orbital, additional holes doped into the planes will primarily reside on the Oxygens. The maximal gain in hybridization energy is achieved by placing the additional hole in a combination of the surround-

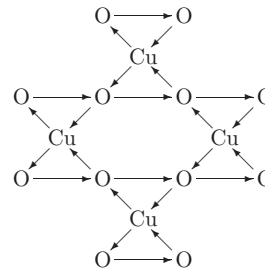


FIG. 1: Orbital current pattern proposed by Varma.

ing O  $2p_x$  and  $2p_y$  orbitals with the same symmetry as the original hole in the Cu  $3d_{x^2-y^2}$  orbital, which requires antisymmetry of the wave function in spin space, *i.e.*, the two holes must form a singlet. This picture is strongly supported by data from NMR<sup>33</sup> and even more directly from spin-resolved photoemission<sup>34</sup>. In the effective one-band  $t$ - $J$  model description of the CuO planes, these singlets constitute the “holes” moving in a background of spin 1/2 particles localized at the Cu sites.

In contrast to this picture, Varma<sup>9,10</sup> has proposed that the additional holes doped in the CuO planes do not hybridize into Zhang-Rice singlets, but give rise to circular currents on O-Cu-O triangles, which align into a planar pattern as shown in Fig. 1. He assumes that the inter-atomic Coulomb potential  $V_{pd}$  is larger than both the hopping  $t_{pd}$  and the on-site potential  $\epsilon_p$  of the O  $2p$  orbitals relative to the Cu  $3d_{x^2-y^2}$  orbitals, an assumption which is not consistent with the values generally agreed on (see the list below (1)). Making additional assumptions, Varma has shown that the circular current patterns are stabilized in a mean field solution of the three-band Hubbard model. The orbital current patterns break time-reversal symmetry (T) and the discrete four-fold rotation symmetry on the lattice, but leave translational symmetry intact. The current pattern is assumed to disappear at a doping level of about  $x_c \approx 0.19$ . The phenomenology of CuO superconductors, including the pseudogap and the marginal Fermi liquid phase, are assumed to result from critical fluctuations around this QCP, as outlined above.

Motivated by this proposal, several experimental groups have looked for signatures of orbital currents or T violation in CuO superconductors. While there is no agreement between different groups regarding the manifestation of T violation in ARPES studies<sup>35,36</sup>, a recent neutron scattering experiment by Fauqué *et al.*<sup>12</sup> indicates magnetic order within the unit cells of the CuO planes. Their results appear to be consistent with Varma’s proposal, and call the validity of the one-band models into question. In a recent article, Aji and Varma<sup>37</sup> have mapped the four possible directions of the current patterns in each unit cell onto two Ising spins, and investigated the critical fluctuations. Within this framework, the couplings between and the transverse fields for these Ising spins effect whether or under which circumstances the model displays long-range order in the orbital currents.

We hence intended to estimate these couplings through numerical studies of finite clusters containing 8 unit cells, *i.e.*, 8 Cu and 16 O sites, and periodic boundary conditions (which do not frustrate but should enhance the correlations). The total number of holes on our cluster was taken  $N = 9$  (5 up-spins and 4 down-spins), corresponding to a hole doping of  $x = 1/8$ . We had hoped that the energy associated with a domain wall, which may be implemented through a twist in the boundary conditions, would provide information regarding the coupling aligning the orbital currents in neighboring plaquets, while the splitting between the lowest energies for a finite system would provide an estimate for the transverse field. Together, this would account for a description of the system in terms of Ising-type variables where the quantum critical behavior could be analyzed.

We find, however, that the current-current correlations in the ground state show no tendency to align the orbital currents whatsoever. There is not even a context to speak of a coupling of these Ising variables—or, in other words, the couplings are zero within the error bars of our numerical experiments.

### III. THREE-BAND MODEL FOR THE CUPRATES

To begin with, we wish to study the three-band Hubbard Hamiltonian  $H = H_t + H_U$  with<sup>38</sup>

$$\begin{aligned}
H_t &= \sum_{i,\sigma} \epsilon_p n_{i,\sigma}^p - t_{pd} \sum_{\langle i,j \rangle, \sigma} \left( d_{i,\sigma}^\dagger p_{j,\sigma} + p_{j,\sigma}^\dagger d_{i,\sigma} \right) \\
&\quad - t_{pp} \sum_{\langle i,j \rangle, \sigma} \left( p_{i,\sigma}^\dagger p_{j,\sigma} + p_{j,\sigma}^\dagger p_{i,\sigma} \right) + V_{pd} \sum_{\langle i,j \rangle, \sigma, \sigma'} n_{i,\sigma}^d n_{j,\sigma'}^p, \\
H_U &= U_p \sum_i n_{i,\uparrow}^p n_{i,\downarrow}^p + U_d \sum_i n_{i,\uparrow}^d n_{i,\downarrow}^d,
\end{aligned} \tag{1}$$

where  $\langle , \rangle$  indicates that the sums extend over pairs of nearest neighbors, while  $d_{i,\sigma}$  and  $p_{j,\sigma}$  annihilate holes in Cu  $3d_{x^2-y^2}$  or O  $2p$  orbitals, respectively. Hybertsen *et al.*<sup>27</sup> calculated  $t_{pd} = 1.5$ ,  $t_{pp} = 0.65$ ,  $U_d = 10.5$ ,  $U_p = 4$ ,  $V_{pd} = 1.2$ , and  $\epsilon_p = 3.6$ , which is the first three-band model discussed below.

In order to be able to diagonalize (1) for a cluster of 24 sites, *i.e.*, 8 Cu and 16 O sites, with 5 up-spin and 4 down-spin holes, we need to truncate the Hilbert space. A first step is to eliminate doubly occupied sites. This yields the effective three-band  $t$ - $J$  Hamiltonian

$$\begin{aligned}
H_{\text{eff}} &= \tilde{P}_G H_t \tilde{P}_G + H_J \quad \text{with} \\
H_J &= J_{pd} \sum_{\langle i,j \rangle} \left( \mathbf{S}_i^p \cdot \mathbf{S}_j^d - \frac{1}{4} \right) + J_{pp} \sum_{\langle i,j \rangle} \left( \mathbf{S}_i^p \cdot \mathbf{S}_j^p - \frac{1}{4} \right),
\end{aligned} \tag{2}$$

where

$$J_{pd} = 2t_{pd}^2 \left( \frac{1}{U_d - \epsilon_p} + \frac{1}{U_p + \epsilon_p} \right), \quad J_{pp} = \frac{4t_{pp}^2}{U_p},$$

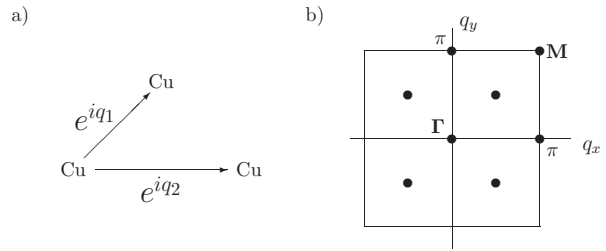


FIG. 2: We define the phases  $q_1$  and  $q_2$  acquired by translations shown in a). For a system of eight unit cells, *i.e.*, 8 Cu and correspondingly 16 O, the phases can have the values  $q_1 = n_1\pi/2$  and  $q_2 = n_2\pi$  with  $n_1 \in \{0, 1, 2, 3\}$  and  $n_2 \in \{0, 1\}$ . For the Brillouin zone depicted in b),  $q_1$  and  $q_2$  translate into  $x$  and  $y$  momenta by  $q_x = q_1$  and  $q_y = q_1 - q_2$ . Thus, the phase description  $(q_1, q_2)$  of the  $\Gamma$  and  $M$  point is  $(0, 0)$  and  $(\pi, 0)$ , respectively.

and the sums in  $H_J$  are limited to pairs where both neighbors are occupied by holes. If  $\tilde{P}_G$  only eliminates configurations with more than one hole on a site, *i.e.*, a pure Gutzwiller projection, the dimension of the  $S_{\text{tot}}^z = \frac{1}{2}$  subsector is 164,745,504, which as such is above our capabilities.

As a next step, we exploit the translational symmetries on the cluster, a 4-fold symmetry in  $\hat{q}_1$  direction and a 2-fold symmetry in  $\hat{q}_2$  direction according to the conventions given in Fig. 2. (Throughout this article, we label the momenta by  $(q_1, q_2)$  rather than  $(q_x, q_y)$ .) The reduced dimension  $\sim 2 \cdot 10^8$  is still a considerably large Hilbert space. Thus, we take two further steps. First, we identify the ground state in the Brillouin zone. As it turns out, for all parameter choices discussed in this article, the respective ground state is either at the  $\Gamma$  or  $M$  point. Second, we apply the rotation symmetry, which commutes with the translational symmetries at and only at the  $M$  and  $\Gamma$  point. The system then becomes amenable to exact diagonalization.

In order to identify the momentum of the ground state, we introduce two ways of truncating the Hilbert space: (a) We limit the maximal number of holes allowed in the O orbitals to  $N_{\text{ox}}^{\text{max}}$ . (b) We limit the maximal number of CuO links occupied with 2 holes to  $N_{\text{link}}^{\text{max}}$ . Truncation (a) serves as a good scheme when the on-site potential  $\epsilon_p$  is large compared to other parameter scales, but is not practicable in other cases. Since truncation (b) predominantly projects out states with high kinetic energy, we expect it to be insensitive to the value of  $\epsilon_p$ . To check the validity of the truncations, we consider Hamil-

$N_{\text{ox}}^{\text{max}}$	(0,0)	$(\frac{\pi}{2}, 0)$	$(\pi, 0)$	$(0, \pi)$
3	-0.7025	-0.6948	-0.7051	-0.6924
4	-0.8256	-0.8204	-0.8350	-0.8198
5	-0.8719	-0.8611	-0.8774	-0.8617

TABLE I: Ground state energies per unit cell for  $\epsilon_p = 3.6$ ,  $V_{pd} = 1.2$  for the inequivalent points in the Brillouin zone and truncation (a).

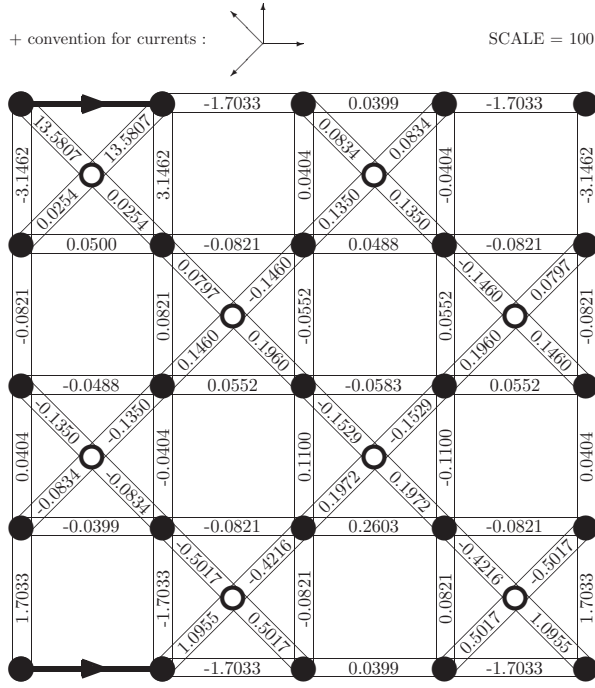


FIG. 3: Current-current correlations  $\langle j_{k,k+\hat{x}} j_{l,m} \rangle$  multiplied by  $10^2$  and in units of  $\frac{\epsilon_V}{\hbar}$  for the ground state of (2) with  $\epsilon_p = 3.6$ ,  $V_{pd} = 1.2$  on a 24 site cluster (8 Cu = open circles, 16 O = filled circles) with PBCs. The reference link is indicated in the top and (due to the PBCs) bottom left corner. Except for the vertical lines, positive numbers indicate alignment with the pattern shown in Fig. 1.

tonian (2) with the parameter values by Hybertsen *et al.* listed above and calculate the ground state energies of the system (see Table I and II).

Both truncation schemes yield similar results. The ground state is situated at the M point  $(\pi, 0)$  of the Brillouin zone. At this point, it is possible to implement a 4-fold rotation symmetry, which commutes with the translational symmetries. Thus, the dimension is reduced by an additional factor of 4 and the exact state is accessible. We find the energies  $E_{(\pi,0,0)} = -0.8513$ ,  $E_{(\pi,0,\pi/2)} = -0.8570$ , and  $E_{(\pi,0,\pi)} = -0.8883$ , where the first two indices label the linear momenta  $(q_1, q_2)$ , and the third labels the angular momentum under discrete rotations by  $90^\circ$ ,  $q_{\text{rot}} = n_{\text{rot}}\pi/4$ , with  $n_{\text{rot}} \in \{0, 1, 2, 3\}$ . The ground state is hence in the  $(\pi, 0, \pi)$  subspace.

$N_{\text{link}}^{\text{max}}$	(0,0)	$(\frac{\pi}{2},0)$	$(\pi,0)$	(0, $\pi$ )
2	0.0640	0.0693	0.0631	0.0715
3	-0.6285	-0.6224	-0.6351	-0.6215
4	-0.8473	-0.8356	-0.8520	-0.8359

TABLE II: Ground state energies per unit cell for  $\epsilon_p = 3.6$ ,  $V_{pd} = 1.2$  for the inequivalent points in the Brillouin zone and truncation (b).

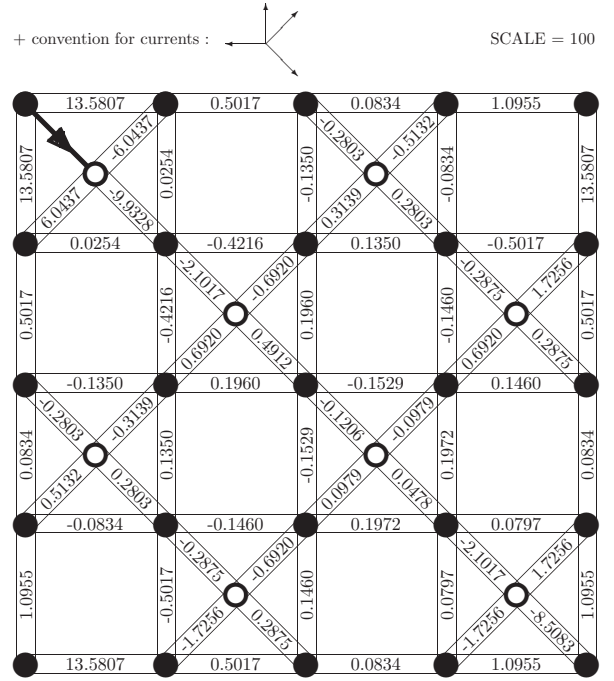


FIG. 4: Current-current correlations  $\langle j_{k,k+\hat{x}} j_{l,m} \rangle$  multiplied by  $10^2$  for the ground state of (2) with  $\epsilon_p = 3.6$ ,  $V_{pd} = 1.2$  on a 24 site cluster (8 Cu = open circles, 16 O = filled circles) with PBCs. The Cu-O reference link is indicated in the top corner.

#### IV. CURRENT-CURRENT CORRELATIONS AND MAGNETIC MOMENTS

With the current operator for an O-O and a Cu-O link given by

$$j_{k,l} = \frac{it_{pp}}{\hbar} \sum_{\sigma} (p_{l,\sigma}^{\dagger} p_{k,\sigma} - p_{k,\sigma}^{\dagger} p_{l,\sigma}) \quad (3)$$

and

$$j_{k,l} = \frac{it_{pd}}{\hbar} \sum_{\sigma} (p_{l,\sigma}^{\dagger} d_{k,\sigma} - d_{k,\sigma}^{\dagger} p_{l,\sigma}), \quad (4)$$

respectively, we evaluated the correlation function  $\langle j_{k,k+\hat{x}} j_{l,m} \rangle$  with O-O and Cu-O links as reference links for the exact ground state. The results are shown in Figs. 3 and 4. The correlations fall off rapidly and there is no indication of order.

We now use the correlations to reach a conclusion regarding the existence or non-existence of the orbital current pattern, indicated in Fig. 1. The numerical experiments for the finite cluster can, as a matter of principle, never rule out directly that a symmetry, in our case time reversal symmetry  $T$ , is violated. As only real parameters enter the Hamiltonian, the computed ground states are real by construction and do not allow for a direct indication of time reversal symmetry breaking. If it were to exist, the computed ground state would be a symmetric superposition of the different separately  $T$  violating ground

states, which itself is T symmetric again and described by a real wave function. The current-current correlation function, however, allows to put an upper bound on the size of the spontaneous currents: If a current pattern as sketched in Fig. 1 were to exist, the current-current correlations  $\langle j_{k,k+\hat{x}} j_{l,l+\hat{x}} \rangle$  for links far away from each other in a rotationally invariant ground state should approach  $\frac{1}{2} \langle \hat{x} | j_{k,k+\hat{x}} | \hat{x} \rangle^2$ , where  $|\hat{x}\rangle$  denotes a state with a spontaneous current pointing in  $\hat{x}$  direction (the factor  $\frac{1}{2}$  arises because by choosing our reference link in  $x$ -direction, we effectively project onto two of the four possible directions for the current pattern). From the values of  $10^2 \cdot \langle j_{k,k+\hat{x}} j_{l,l+\hat{x}} \rangle$  for the four horizontally connected links in the center of Fig. 3,  $-0.0488, +0.0552, -0.0583$ , and  $+0.0552$ , which should all be positive if a current pattern were present, we estimate  $10^2 \cdot \langle j_{k,k+\hat{x}} \rangle^2 < 0.05$  and hence  $\langle \hat{x} | j_{k,k+\hat{x}} | \hat{x} \rangle^2 < 1 \cdot 10^{-3}$  as an upper bound for a current pattern we are unable to detect through the error bars of our numerical experiment. (Throughout this article, currents are quoted in units of  $\text{eV}/\hbar$ .) We now denote  $\langle \hat{x} | j_{k,k+\hat{x}} | \hat{x} \rangle$  by  $j_{\text{pp}}$ .

We roughly estimate the kinetic energy  $\varepsilon_{\text{pp}}$  per link associated with a spontaneous current  $j_{\text{pp}}$  of this magnitude using  $j_{\text{pp}} = n_{\text{p}} v$  and  $\varepsilon_{\text{pp}} = \frac{1}{2} n_{\text{p}} m v^2$  with  $m = 1/2t_{\text{pp}}$ , where  $n_{\text{p}}$  is the hole density on the Oxygen sites ( $n_{\text{p}} = 0.14$  for the state analyzed in Fig. 3), and obtain

$$\varepsilon_{\text{pp}} \approx \frac{\hbar^2 j_{\text{pp}}^2}{4t_{\text{pp}} n_{\text{p}}} < 3 \cdot 10^{-3}. \quad (5)$$

A similar analysis with a Cu-O reference link (shown in Fig. 4) yields with  $10^2 \cdot \langle j_{k,k+\hat{x}+\hat{y}} \rangle^2 < 1.0$  and hence  $j_{\text{pd}}^2 < 10^{-2}$  (there is no factor  $\frac{1}{2}$  in this case) an estimate of

$$\varepsilon_{\text{pd}} \approx \frac{\hbar^2 j_{\text{pd}}^2}{4t_{\text{pd}} \sqrt{n_{\text{p}} n_{\text{d}}}} < 5 \cdot 10^{-3}, \quad (6)$$

where we have determined  $n_{\text{d}}$  via  $8n_{\text{d}} + 16n_{\text{p}} = 9$ .

Note that this energy of 3 (or 5) meV is not the condensation energy  $E_{\text{c}}$  per unit cell, but a positive contribution to the energy of the current carrying state, which would have to be (more than) offset by other contributions (like the energy gain from aligning the circulating currents according to the pattern Varma proposed) if such a state were realized. We would expect the transition temperature  $T_{\text{c}}$  of such a state to be of the order of the effective coupling of the Ising spins introduced by Aji and Varma<sup>37</sup>, while we would expect that  $E_{\text{c}} \ll T_{\text{c}}$ .

Making contact to the quantities observed in experiment, we now derive an upper bound of the magnetic moment from the upper bound for the spontaneous currents we obtained through numerics. The magnetization is related to the angular momentum of circulating electrons by  $M = -\mu_{\text{B}} L_z / \hbar$  with  $L_z = m_e r v$ , where  $r$  denotes the distance to the center of rotation and  $v$  the velocity of the electrons.

With a Cu-Cu distance  $a_0 \approx 3.8\text{\AA}$ , the side lengths of the isosceles O-Cu-O triangle are  $\frac{a_0}{2}$  for the two equal

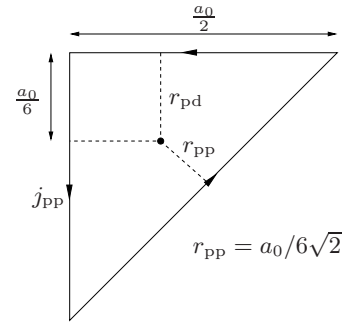


FIG. 5: Circulating current  $j_{\text{pp}}$  on a neighboring O triangle according to the pattern in Fig. 1. Lengths are given in units of the Cu-Cu distance  $a_0$ .

legs and  $\frac{a_0}{\sqrt{2}}$  for the third side, as shown in Fig. 5. The distance of the sides to the center-of-mass point are given by  $r_{\text{pd}} = \frac{a_0}{6}$  and  $r_{\text{pp}} = \frac{a_0}{6\sqrt{2}}$ . Given the upper bound on the current-current correlations  $10^2 \langle \hat{x} | j_{k,k+\hat{x}} | \hat{x} \rangle^2 \lesssim 0.1 \left(\frac{\text{eV}}{\hbar}\right)^2$ , we infer a bound for the particle current

$$j_{\text{pp}} < 0.03 \frac{\text{eV}}{\hbar}. \quad (7)$$

Note that the units correspond to 1/time ( $1\text{eV}/\hbar = 1.517 \times 10^{15} \text{ 1/s}$ ). Assuming that each triangle is occupied by 1 hole only, this current corresponds classically to the inverse time the hole takes to go around the triangle once.

Assuming further that the hole dwells equal amounts of time on each link defining the triangle, the velocity on the O-O link is given by

$$v_{\text{pp}} = \frac{a_0}{\sqrt{2}} / \left( \frac{1}{3} \frac{1}{j_{\text{pp}}} \right) = \frac{3a_0}{\sqrt{2}} j_{\text{pp}}$$

and on the Cu-O links by

$$v_{\text{pd}} = \frac{a_0}{2} / \left( \frac{1}{3} \frac{1}{j_{\text{pp}}} \right) = \frac{3a_0}{2} j_{\text{pp}}$$

With  $L_z = m_e r_{\text{pp}} v_{\text{pp}} = m_e r_{\text{pd}} v_{\text{pd}}$ , we find an upper bound for the associated angular momentum

$$L_z^{\text{pp}} \lesssim 0.015 \hbar. \quad (8)$$

As there are two current carrying triangles per unit cell in the pattern shown in Fig. 1, we find an upper bound of the magnetic moment induced by the currents:

$$M_{\text{cell}} = 2M_{\Delta} \lesssim 0.03 \mu_{\text{B}}. \quad (9)$$

The result is below the estimate of  $M \approx 0.05\text{--}0.1\mu_{\text{B}}$  found experimentally by Fauqué *et al.*<sup>12</sup>. (As we lower  $\varepsilon_{\text{p}}$  in Section VI below, however, the upper bound for  $j_{\text{pp}}$  and  $j_{\text{pd}}$  we are able to obtain from our numerical experiments increase, and becomes comparable to the experimental estimate.)

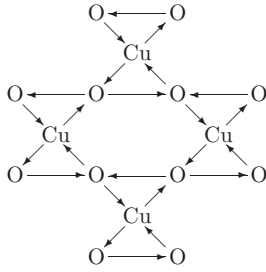


FIG. 6: An orbital current pattern proposed earlier by Varma, which has subsequently been ruled out by experiment.

This provides an interesting perspective on the strength of the magnetic moment observed in the experiment. If a pattern as shown in Fig. 1 were responsible for this moment, the associated current would be in a range of  $\sim 0.05 - 0.1$  eV/ $\hbar$ , a signal strength which we do not observe in the numerics. Even if currents of this magnitude were present in the CuO layers, however, following the previous derivation, the energy associated with this current strength would only be in the range of 10 – 30 meV and thus too small to explain the phase diagram of the high- $T_c$  cuprates. This suggests that even if orbital current alignment were responsible for the magnetic moment measured in experiments, these currents would not be sufficiently large to account for the strange metal phenomenology of high- $T_c$  superconductivity.

The immediate conclusion we draw from our numerical results, however, is that if the CuO planes are adequately described by a three-band model with a set of couplings in the range we investigated, the antiferromagnetic ordering observed by Fauqué *et al.*<sup>12</sup> is not due to an orbital current pattern as shown in Fig. 1. We are hence led to ponder whether our models might be consistent with an alternative explanation of this experiment. The correlations we observe would be consistent with another orbital current pattern, shown in Fig. 6, which had been proposed by Varma earlier<sup>9,10</sup>. This pattern, however, has been successfully ruled out by neutron scattering experiment<sup>39</sup>, and is not consistent with the experiment of Fauqué *et al.*<sup>12</sup>. The correlations we observe, on the other hand, provide no indication that such a pattern is realized, as our system sizes are way too small to establish the existence of any kind of long range order. We are merely not able to rule out order according to this pattern with our numerical data. Considering the possibility of this pattern being realized, however, does in any event not bring us closer to understanding the magnetic moment observed by Fauqué *et al.*<sup>12</sup>.

## V. SPIN-SPIN CORRELATIONS

If the observed magnetic moment is not due to orbital currents, what other possibilities are there? The only other explanation which comes to mind within the confines of our three-band models is antiferromagnetic order of the spins on the Oxygen lattice. The characteristic

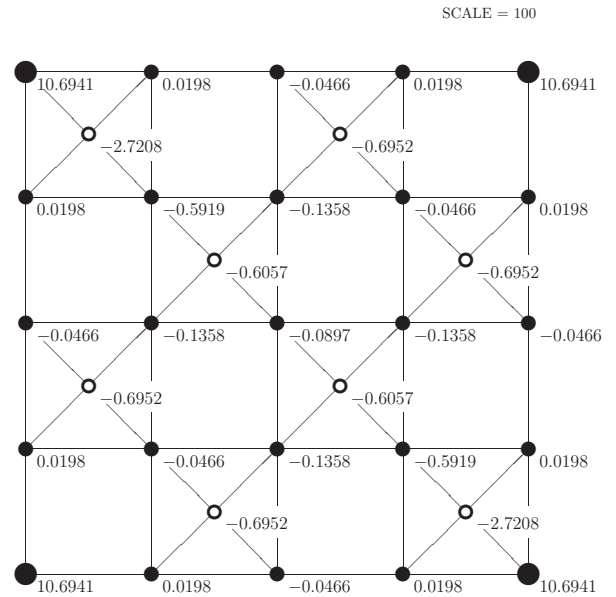


FIG. 7: Spin-spin correlations multiplied by  $10^2$  for the ground state of (2) with  $\epsilon_p = 3.6$ ,  $V_{pd} = 1.2$  on a 24 site cluster (8 Cu = open circles, 16 O = filled circles). Due to PBCs the O reference site is in all corners of the plot and indicated by a big black circle.

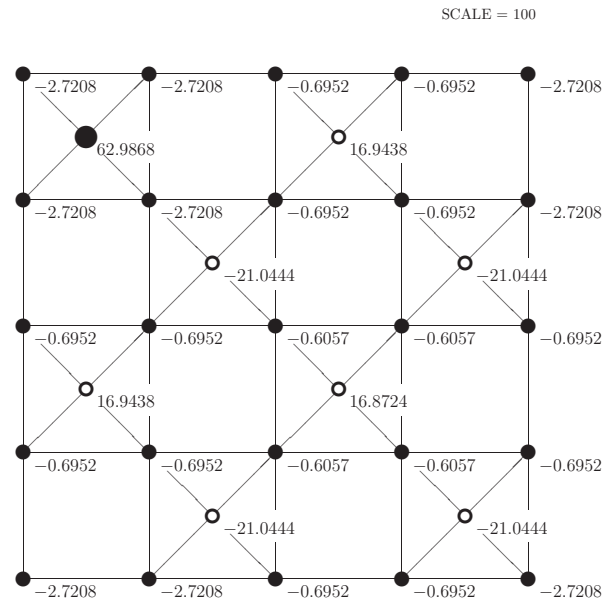


FIG. 8: Spin-spin correlations multiplied by  $10^2$  for the ground state of (2) with  $\epsilon_p = 3.6$ ,  $V_{pd} = 1.2$  with PBCs. The Cu reference site to the upper left is indicated by a big black circle.

term driving the system into this kind of order would be the antiferromagnetic coupling  $J_{pp}$  in our effective Hamiltonian (2). According to our intuition about the system, there is no reason to expect this kind of order, but as it is straightforward to obtain the spin-spin correlations for our finite cluster, we discuss them briefly in this section.

We have evaluated the static spin-spin correlation of

spins at sites  $i$  and  $j$  given by

$$\mathcal{S}_{ij} = \left\langle \vec{S}_i \vec{S}_j \right\rangle,$$

with an O or a Cu as reference site. The results are shown in Figs. 7 and 8, respectively. For the O sublattice, we only observe a very small staggered spin correlation which falls off rapidly with distance on the scale of the lattice constant, regardless of whether we choose an O or a Cu as reference site. We do not observe any indication of antiferromagnetic order on the O sites, as the required long range correlations are clearly absent. We will hence not discuss the spin-spin correlations any further and focus on the current-current correlations instead.

Regarding the experiment by Fauqué *et al.*<sup>12</sup>, we believe that the explanation will require a model which goes beyond the projected three-band models studied here. The explanation might, for example, involve orbital currents localized at the O atoms.

## VI. RESULTS FOR DIFFERENT PARAMETER SETTINGS

We now consider various parameter choices for the three-band Hubbard model. The two parameters which

---

We now turn to the different choices for the model parameters. Except for  $\epsilon_p$  and  $V_{pd}$ , we use the three-band Hubbard parameters calculated by Hybertsen *et al.*<sup>27</sup>. We label the different sections by the values for  $\epsilon_p$  and  $V_{pd}$  we specifically investigate.

### A. $\epsilon_p = 1.8, V_{pd} = 1.2$

As we decrease  $\epsilon_p$  from 3.6 to 1.8, the ground state switches from momentum  $(\pi, 0)$  to  $(0, 0)$ , *i.e.*, from the M to the  $\Gamma$  point in the Brillouin zone (see Table III). Implementing the rotational symmetry yields  $E_{(0,0,0)} = -1.4551$ ,  $E_{(0,0,\pi/2)} = -1.4350$ , and  $E_{(0,0,\pi)} = -1.4857$  (see Table IV), *i.e.*, the ground state is at  $(0, 0, \pi)$ . The current-current correlations for this state are depicted in Fig. 9. There is no evidence for a pattern along the lines of Fig. 1. Instead, the correlations decrease rapidly with distance. The “fluctuations” or “noise” inherent in the finite size calculation are comparable to the preceding case  $\epsilon_p = 3.6$ . The values of  $10^2 \cdot \langle j_{k,k+\hat{x}} j_{l,l+\hat{x}} \rangle$  for the four horizontally connected links in the center of Fig. 9,  $+0.0028, +0.0199, -0.0430$ , and  $+0.0199$  indicate no relevant scale of correlations. Recall that the orbital current pattern shown in Fig. 1 would require all the numbers to be positive.

Varma<sup>10</sup> assumed to differ significantly from the values used above are the relative on-site potential  $\epsilon_p$ , which he assumed to be small compared to all other energy scales, and the inter-atomic Coulomb interaction  $V_{pd}$ , which he assumed to be the leading energy scale of the system generating the orbital currents.

Thus, our strategy is as follows. Firstly, we successively decrease  $\epsilon_p$  from 3.6 to 1.8, 0.9, 0.4, and finally 0, and analyze each model as explained above. Secondly, for small values of  $\epsilon_p$ , we double  $V_{pd}$  from the standard value 1.2 to 2.4 and look whether this significantly influences the system. In doing so, we implicitly sweep over a broad range of the charge transfer gap, which is dependent on  $V_{pd}$  and  $\epsilon_{pd}$ . To begin with, we have computed the ground state energies per link for all inequivalent points in the Brillouin zone for all parameter choices we consider (see Table III). We found that the ground states are either situated in the  $\Gamma$  point or M point of the Brillouin zone. This is not surprising as it is plausible that the ground state does not carry any net momentum, and also consistent with the current pattern shown in Fig. 1. For the states at the  $\Gamma$  and the M point, we then implement the rotation symmetry discussed above and compute the ground state energies per link in the respective subspaces exactly. The results are shown in Table IV.

$\epsilon_p$	$V_{pd}$	$(0,0)$	$(\frac{\pi}{2},0)$	$(\pi,0)$	$(0,\pi)$
3.6	1.2	-0.8473	-0.8356	<u>-0.8520</u>	-0.8359
1.8	1.2	<u>-1.4187</u>	-1.3888	-1.4104	-1.3925
0.9	1.2	<u>-1.7852</u>	-1.7508	-1.7732	-1.7569
0.4	1.2	<u>-2.0290</u>	-2.0011	-2.0185	-2.0066
0.4	2.4	<u>-1.6486</u>	-1.6381	-1.6433	-1.6387
0.0	1.2	<u>-2.2543</u>	-2.2427	-2.2438	-2.2407
0.0	2.4	-1.9199	-1.9265	<u>-1.9342</u>	-1.9261

TABLE III: Ground state energies per unit cell for the different momentum subspaces in the  $N_{\text{link}}^{\text{max}} = 4$  approximation. The numbers for the subspace with the lowest energies, corresponding to the ground state of the full Hamiltonian, are underlined.

### B. $\epsilon_p = 0.9, V_{pd} = 1.2$

As we decrease  $\epsilon_p$  further to 0.9, the lowest state remains in the  $\Gamma$  point, *i.e.*,  $(0, 0, \pi)$ . The ground state correlations are depicted in Fig. 10. They fall off less rapidly with distance than for larger values of  $\epsilon_p$ . Again, there is no indication of a current pattern. The values of  $10^2 \cdot \langle j_{k,k+\hat{x}} j_{l,l+\hat{x}} \rangle$  for the four horizontally connected links in the center of Fig. 10,  $-0.420, +0.0338, -0.0647$ , and  $+0.0338$ , indicate likewise no relevant scale of correlations.

$\epsilon_p$	$V_{pd}$	(0,0,0)	(0,0, $\frac{\pi}{2}$ )	(0,0, $\pi$ )	( $\pi$ ,0,0)	( $\pi$ ,0, $\frac{\pi}{2}$ )	( $\pi$ ,0, $\pi$ )
3.6	1.2	-0.8544	-0.8545	-0.8843	-0.8513	-0.8570	<u>-0.8883</u>
1.8	1.2	-1.4551	-1.4350	<u>-1.4857</u>	-1.4462	-1.4448	-1.4769
0.9	1.2	-1.8440	-1.8136	<u>-1.8672</u>	-1.8345	-1.8304	-1.8557
0.4	1.2	-2.0986	-2.0820	<u>-2.1149</u>	-2.0932	-2.0859	-2.1053
0.4	2.4	-1.6864	-1.6788	<u>-1.7007</u>	-1.6950	-1.6741	-1.6923
0.0	1.2	-2.3269	<u>-2.3400</u>	-2.3389	-2.3317	-2.3280	-2.3372
0.0	2.4	-1.9508	-1.9613	-1.9647	<u>-1.9766</u>	-1.9543	-1.9619

TABLE IV: Exact ground state energies for the  $\Gamma$  point (0, 0,  $q_{\text{rot}}$ ), and the M point ( $\pi$ , 0,  $q_{\text{rot}}$ ), with additionally applied rotation symmetry ( $q_{\text{rot}} = 3\pi/2$  is degenerate to  $q_{\text{rot}} = \pi/2$ ). The numbers for the subspace with the lowest energies, corresponding to the ground state of the full Hamiltonian, are underlined.

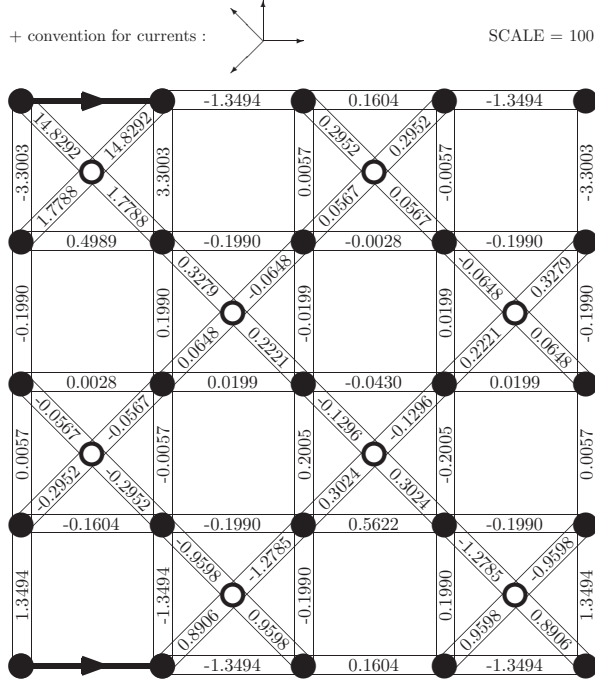


FIG. 9: Current-current correlations  $\langle j_{k,k+\hat{x}} j_{l,m} \rangle$  multiplied by  $10^2$  for the ground state of (2) with  $\epsilon_p = 1.8$ ,  $V_{pd} = 1.2$  on a 24 site cluster with PBCs (reference link indicated in the top and bottom left corner).

### C. $\epsilon_p = 0.4$ , $V_{pd} = 1.2$

The correlations for the ground state, which remains at the (0,0, $\pi$ ) point, are depicted in Fig. 11. We have now reached a parameter regime for which Varma proposed that a current pattern should occur:  $\epsilon_p$  is small compared to  $V_{pd}$ , and  $V_{pd}$  is of the order of the other scales. However, we still find no indication of a current pattern. The values  $10^2 \cdot \langle j_{k,k+\hat{x}} j_{l,l+\hat{x}} \rangle$  for the four horizontally connected links in the center of Fig. 11,  $-0.0971$ ,  $+0.0220$ ,  $-0.0795$ , and  $+0.0220$ , remain small. Nonetheless, let us estimate the energy associated with an upper bound for the currents as elaborated on above. We estimate  $10^2 \cdot \langle j_{k,k+\hat{x}} \rangle^2 < 0.1$  and hence  $\langle \hat{x} | j_{k,k+\hat{x}} | \hat{x} \rangle^2 < 2 \cdot 10^{-3}$  as an upper bound for a uniform

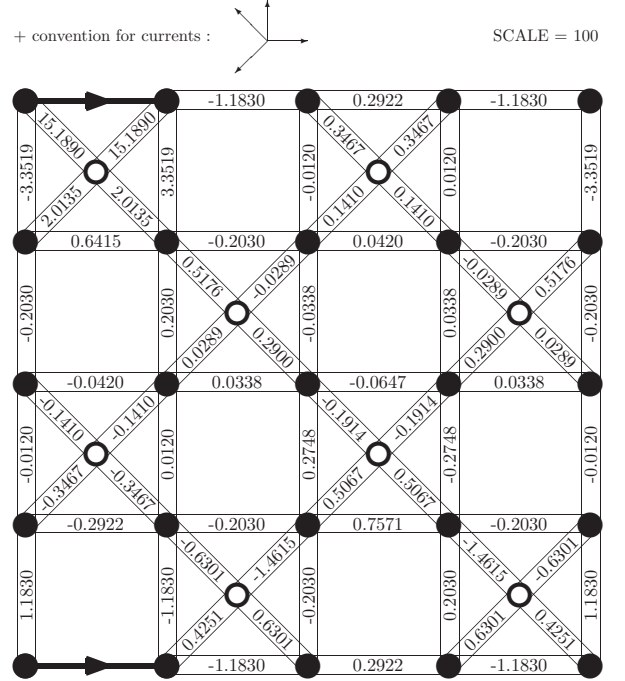


FIG. 10: Current-current correlations  $\langle j_{k,k+\hat{x}} j_{l,m} \rangle$  multiplied by  $10^2$  for the ground state of (2) with  $\epsilon_p = 0.9$ ,  $V_{pd} = 1.2$  on a 24 site cluster with PBCs.

contribution according to a current pattern as depicted in Fig. 1. As above,  $\langle \hat{x} | j_{k,k+\hat{x}} | \hat{x} \rangle$  is denoted by  $j_{pp}$ . For the kinetic energy  $\epsilon_{pp}$  per link associated with a spontaneous current

$$j_{pp} \lesssim 0.05 \frac{eV}{\hbar}$$

we obtain with  $n_p = 0.24$

$$\epsilon_{pp} \approx \frac{\hbar^2 j_{pp}^2}{4t_{pp} n_p} < 3 \cdot 10^{-3}.$$

If a spontaneous currents were hence to exist, the energy associated with them would be too small to allow for an interpretation of the strange metal phase in terms of the quantum critical fluctuations around this phase.



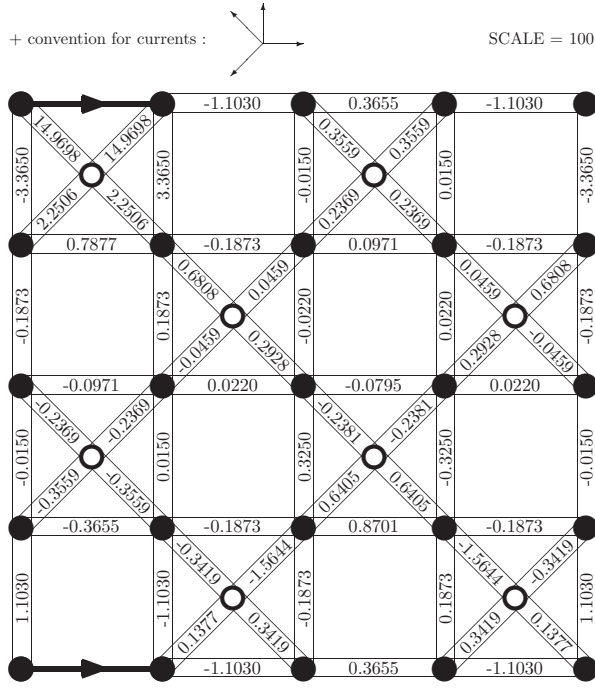


FIG. 11: Current-current correlations  $\langle j_{k,k+\hat{x}} j_{l,m} \rangle$  multiplied by  $10^2$  for the ground state of (2) with  $\epsilon_p = 0.4$ ,  $V_{pd} = 1.2$  on a 24 site cluster with PBCs.

#### D. $\epsilon_p = 0.4$ , $V_{pd} = 2.4$

For  $\epsilon_p = 0.4$ , we have also doubled the Coulomb repulsion between the Cu and O sites to  $V_{pd} = 2.4$ , which then becomes the leading energy scale before the Copper-Oxygen hopping  $t_{pd} = 1.5$ . The ground state remains at the  $\Gamma$  point of the Brillouin zone (see Table III). Compared to  $V_{pd} = 1.2$ , the energies of the  $\Gamma$  and M ground states are now much closer to each other. The correlations for the ground state at  $(0, 0, \pi)$  are shown in Fig. 12. Again, there is no evidence of a current pattern. The values of  $10^2 \cdot \langle j_{k,k+\hat{x}} j_{l,l+\hat{x}} \rangle$  for the four horizontally connected links in the center of Fig. 12,  $-0.1501$ ,  $-0.0487$ ,  $-0.0399$ , and  $-0.0487$ , are comparable to the case  $V_{pd} = 1.2$  discussed above. Note that the four horizontal links we consider are now aligned. Unfortunately, the sign of all four numbers is opposite to the sign required by the pattern shown in Fig. 1.

#### E. $\epsilon_p = 0$ , $V_{pd} = 1.2$

This setting has already been discussed previously<sup>11</sup>. In a sense,  $\epsilon_p = 0$  is the most favorable choice for Varma's mean field approach. It should be kept in mind, however, that  $\epsilon_p$  must be positive and finite in the experimental system to account for the antiferromagnetic order in the undoped cuprates. The ground state is now doubly degenerate and found at  $(0, 0, \pm\pi/2)$ . There is no current pattern observable, but the values of  $10^2 \cdot \langle j_{k,k+\hat{x}} j_{l,l+\hat{x}} \rangle$

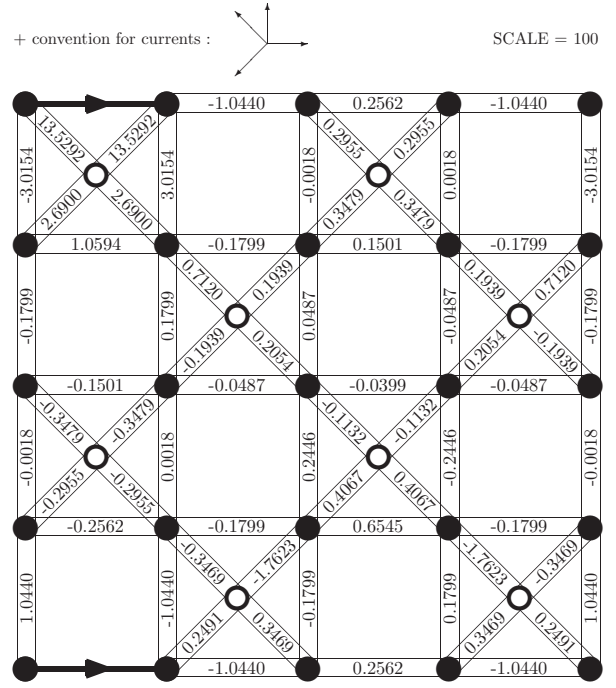


FIG. 12: Current-current correlations  $\langle j_{k,k+\hat{x}} j_{l,m} \rangle$  multiplied by  $10^2$  for the ground state of (2) with  $\epsilon_p = 0.4$ ,  $V_{pd} = 2.4$  on a 24 site cluster with PBCs.

for the four horizontally connected links in the center of Fig. 13,  $0.3726$ ,  $-0.1483$ ,  $-0.4123$ , and  $-0.1483$ , are larger than for any of the other parameter settings we investigated. The uniform current is still zero, but with larger “fluctuations” or “noise” due to the finite size of our system. We estimate an upper bound for a uniform positive correlation  $10^2 \cdot \langle j_{k,k+\hat{x}} \rangle^2 < 0.2$  and hence  $\langle \hat{x} | j_{k,k+\hat{x}} | \hat{x} \rangle^2 < 4 \cdot 10^{-3}$ . As above,  $\langle \hat{x} | j_{k,k+\hat{x}} | \hat{x} \rangle$  is denoted by  $j_{pp}$ , and the approximate kinetic energy  $\epsilon_{pp}$  per link associated with a spontaneous current

$$j_{pp} < 0.06 \frac{eV}{\hbar}$$

yields with (5) and  $n_p = 0.34$ ,

$$\epsilon_{pp} < 5 \cdot 10^{-3}.$$

The correlations with Cu-O reference link are shown in Fig. 14. A similar analysis yields with (6)

$$\epsilon_{pd} < 4 \cdot 10^{-3}.$$

The upper bound of 5 meV we found for the energy associated with spontaneous currents corresponds to a temperature  $T_{\text{current}} \sim 60\text{K}$ . To explain the strange metal phase, however, the energy scale responsible for the quantum critical fluctuations would have to extend at least to a range of several hundred Kelvin.

Note that the upper bound for the magnetic moment per unit cell is now given by

$$M_{\text{cell}} = 2M_{\Delta} \lesssim 0.06 \mu_B, \quad (10)$$

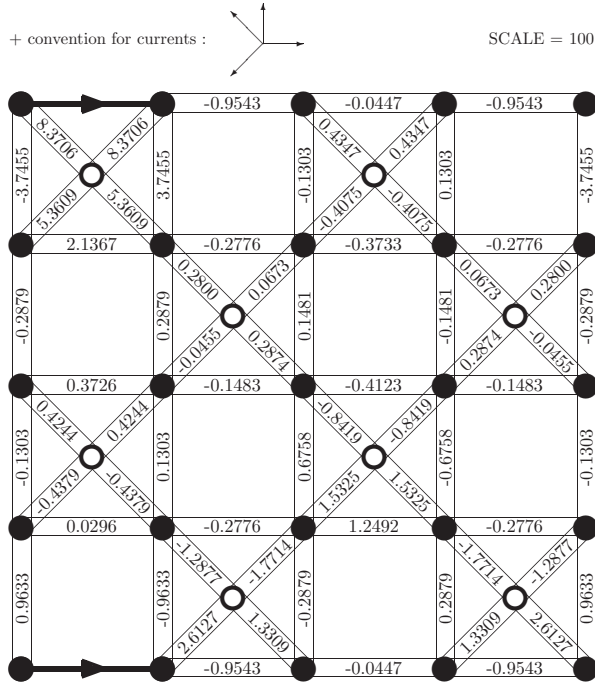


FIG. 13: Current-current correlations  $\langle j_{k,k+\hat{x}} j_{l,m} \rangle$  multiplied by  $10^2$  for the ground state of (2) with  $\epsilon_p = 0.0$ ,  $V_{pd} = 1.2$  on a 24 site cluster with PBCs.

a value roughly comparable to the range of  $M \approx 0.05\text{--}0.1\mu_B$  found experimentally by Fauqué *et al.*<sup>12</sup>. This does not imply that these orbital currents exist, but only states that if we assume a three band model with  $\epsilon_p = 0$ , we are not able to rule out an orbital current pattern as shown in Fig. 1 as an explanation for the experimentally observed magnetic moment. On the other hand, even if the observed moments are due to such a pattern, the energies involved are too small to explain the phenomenology of the strange metal phase.

#### F. $\epsilon_p = 0$ , $V_{pd} = 2.4$

Finally, we double the repulsion  $V_{pd}$  for  $\epsilon_p = 0$ . The ground state is now at the M point, at  $(\pi, 0, 0)$  (see Tab. IV). The corresponding correlations are shown in Fig. 15. Again, there is no evidence for a current pattern. The values of  $10^2 \cdot \langle j_{k,k+\hat{x}} j_{l,l+\hat{x}} \rangle$  for the four horizontally connected links in the center of Fig. 15, 0.0909,  $-0.0885$ , 0.0865, and  $-0.0885$ , are rather small. We estimate an upper bound  $10^2 \cdot \langle j_{k,k+\hat{x}} \rangle^2 < 0.1$  and hence  $\langle \hat{x} | j_{k,k+\hat{x}} | \hat{x} \rangle^2 < 2 \cdot 10^{-3}$  for the contribution from spontaneous currents. For the associated kinetic energy  $\epsilon_{pp}$  per link we find with  $n_p = 0.36$

$$\epsilon_{pp} < 2 \cdot 10^{-3}.$$

Note that since  $V_{pd}$  is driving the orbital currents in the mean field theory proposed by Varma<sup>10</sup>, his theory would predict the model to show the strongest propensity to

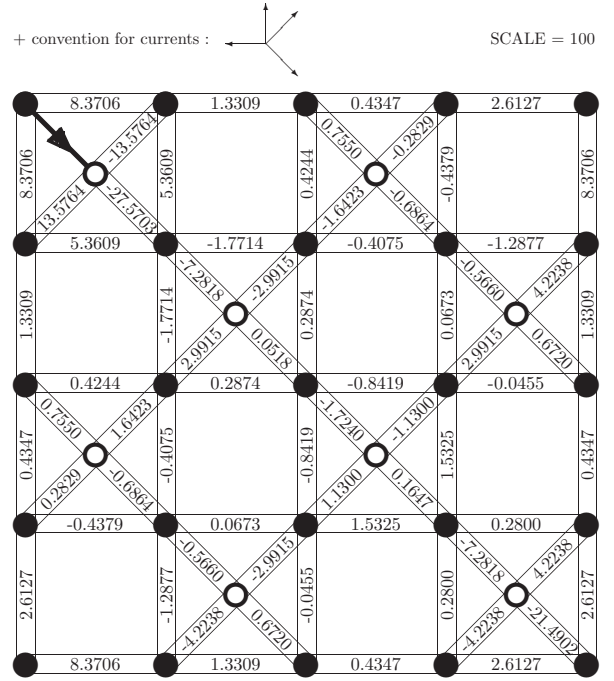


FIG. 14: Current-current correlations  $\langle j_{k,k+\hat{x}} j_{l,m} \rangle$  multiplied by  $10^2$  for the ground state of (2) with  $\epsilon_p = 0.0$ ,  $V_{pd} = 1.2$  on a 24 site cluster with PBCs. The Cu-O reference link is indicated by a black arrow in the upper left corner.

form current patterns for this choice of parameters. By contrast, we find no indication of such a propensity in our numerical experiments.

## VII. FINITE SIZE EFFECTS

The numerical calculations we report here were performed on a cluster of 8 unit cells, *i.e.*, 24 sites (8 Copper and 16 Oxygen). The question we wish to address in this section is whether any of the finite size effects might affect our overall conclusion. Due to the finite size, we have not been able to measure the current-current correlations at long distances, where they would accurately provide the size of a spontaneous current if such a current were to exist. Instead, we have only been able to establish upper bounds on such currents. These upper bounds, however, turned out to be small enough to allow us to rule out that an orbital current pattern as proposed by Varma and shown in Fig. 1 is responsible for the anomalous properties of the strange metal phase in the cuprates.

There are, however, two other finite size effects which may limit the validity of our conclusion. The first is that the ground states in our systems have spin  $S = 1/2$ , as we have a total of 9 holes, corresponding to a doping of one hole away from half filling. The current carrying state proposed and investigated by Varma, by contrast, is in general a spin singlet. Could it be that the extra spin 1/2 destroys the orbital current pattern in our numerical

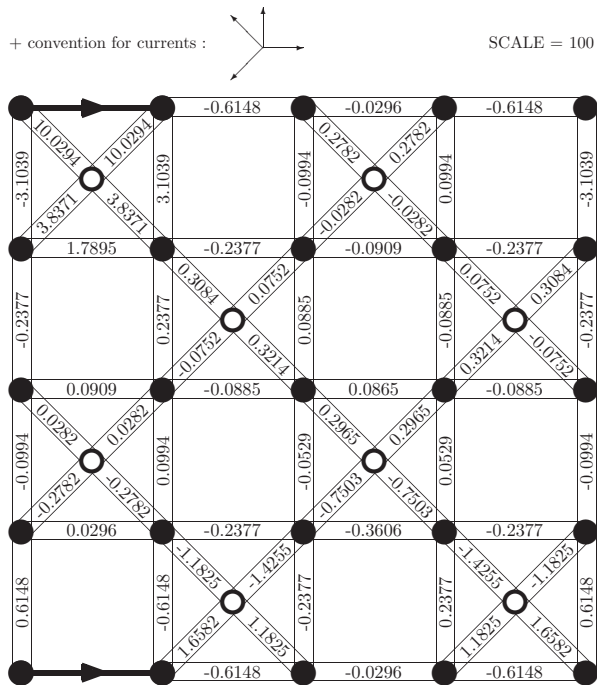


FIG. 15: Current-current correlations  $\langle j_{k,k+\hat{x}} j_{l,m} \rangle$  multiplied by  $10^2$  for the ground state of (2) with  $\epsilon_p = 0.0$ ,  $V_{pd} = 2.4$  on a 24 site cluster with PBCs.

experiments, while the currents would be present if we had an infinite system? We will argue now that any possible effect would not affect our conclusions.

To begin with, assuming that no magnetic spin order is present, the ground state of the infinite system will be a spin singlet, regardless of whether the state carries a spontaneous current or not. This also holds for any finite system with an even number of electrons, even if long range antiferromagnetic correlations in the spins were present. The ground state for a finite system with an odd number of electrons, as we have investigated in this work, will correspond to the ground state for an even number of electrons supplemented by an excitation which carries spin 1/2. This excitation will cost a finite amount of energy. The question relevant for the validity of our conclusion is whether the energy cost of this spin 1/2 excitation is higher for a current carrying state than it is for a state without currents, and if it is higher, by which amount. Since the term driving the spontaneous currents in Varma’s analysis is  $V_{pd}$ , the energy associated with this term has to be lower in the current carrying state, while we would expect most other terms in the Hamiltonian, but in particular the antiferromagnetic exchange terms  $J_{pd}$  and  $J_{pp}$ , to be slightly higher in energy. As the excitation energy for the extra spin 1/2 amounts mostly to an extra energy cost in  $J_{pd}$  and  $J_{pp}$ , we expect that this excitation will cost less energy in the current carrying state than in the state without currents. In other words, unless the antiferromagnetic exchange terms in (1) were to contribute towards driving the system into a current carrying phase, the spin 1/2 excitation in our finite sys-

tem would enhance the stability of this phase. The fact that we do not observe a current pattern in the presence of the extra spin 1/2 makes our conclusion even more robust than it would be without the excitation.

To rule out any doubt completely, let us be unreasonable and assume that the antiferromagnetic exchange terms do in fact enhance the systems propensity to develop spontaneous currents, and that the antiferromagnetic exchange energy in the current carrying phase is maybe about 10% below the energy of the phase without the currents. For the parameter choice  $\epsilon_p = 0$  and  $V_{pd} = 1.2$ , the antiferromagnetic exchange energy per unit cell is

$$\epsilon_J = \frac{1}{8} \langle \Psi_0 | H_J | \Psi_0 \rangle = 122 \text{ meV}, \quad (11)$$

with  $H_J$  given in (2). To estimate the energy cost of the spin 1/2 excitation, we compare the ground state energy for  $S = 1/2$  obtained for 5 up and 4 down spin holes with the ground state energy for  $S = 3/2$  obtained for 6 up and 3 down spin holes, and find an energy difference of  $\Delta = 230$  meV. Since the ground state energy for the different spin sectors should roughly be proportional to  $S^2$ , the energy cost of the  $S = 1/2$  excitation should be roughly 1/8th of this difference, or about 30 meV. The energy cost of the excitation per unit cell of our finite cluster is hence of the order of 4 meV. If we now assume that the energy cost for this  $S = 1/2$  excitation increases by 10% if spontaneous currents are present (the cost increases because the excitation disturbs the current driving antiferromagnetic correlations), the additional energy cost for the currents due to the extra spin 1/2 would be of order 0.4 meV per unit cell, or roughly 0.04 meV per link. If this energy cost were to destabilize the spontaneous currents, the energy associated with them would be below the upper bounds estimated from the current-current correlations above.

The second finite size effect we briefly wish to mention is that the special geometry of periodic boundary conditions might have an unintended influence on the system, maybe in that it stabilizes a state without currents which would not be stable in the infinite system. We have hence twisted and varied the boundary conditions in any way we could think of, but found that the correlations, and in particular the “fluctuation” or “noise level” due to the finite size which limits or ability to put upper bounds on the correlations, remained unchanged.

## VIII. CONCLUSION

Let us summarize the results of our numerical studies on three-band Hubbard models for the cuprate planes in CuO superconductors. For the commonly accepted parameter values as calculated by Hybertsen<sup>27</sup>, we find no orbital current pattern as shown in Fig. 1 as well as no significant antiferromagnetic spin-spin correlation on the Oxygen sites. As we sweep over a considerable parameter regime of  $\epsilon_p$  and  $V_{pd}$  and compute the current-current

correlations for the respective ground states, we likewise do not observe any evidence for a pattern as advocated by Varma's mean field analysis. Instead, we find that the correlations change quantitatively, but not qualitatively, as we move through the parameter space. We also observe that there is no clear dependence of the correlations on  $V_{pd}$ , which is not consistent with what one would expect from Varma's analysis. We conclude that while we cannot rule out that orbital current patterns exist, we can rule out that they are responsible for the properties of the strange metal phase or the anomalous normal state properties extending up to temperatures of several hundred Kelvin, as the energy associated with the spontaneous loop currents would be less than 5 meV per link if such currents were to exist. We have assumed that the CuO planes are adequately described by the three-band Hubbard model (1), but we have allowed  $\epsilon_p$  to be much smaller and  $V_{pd}$  larger than generally agreed upon, and

based our estimate for the upper bound of 5 meV on the for our purposes most unfavorable case  $\epsilon_p = 0$ .

### Acknowledgments

We wish like to thank C.M. Varma, V. Aji, F. Evers, and in particular P. Wölfle for many illuminating discussions of this subject. RT was supported by a PhD scholarship from the Studienstiftung des deutschen Volkes. We further acknowledge the support of the computing facilities of the INT at the Forschungszentrum Karlsruhe.

*Note added:* After this work was completed, we learned of a slave boson mean field calculation by Kremer, Brinckmann, and Wölfle<sup>40</sup>, who likewise found no spontaneous currents in the ground state of the model originally analyzed by Varma.

- 
- <sup>1</sup> J. G. Bednorz and K. A. Müller, *Zeitschrift für Physik B Condensed Matter* **64**, 189 (1986).  
<sup>2</sup> J. Zaanen *et al.*, *Nature Physics* **2**, 138 (2006).  
<sup>3</sup> P. W. Anderson, *Science* **235**, 1196 (1987).  
<sup>4</sup> P. A. Lee, N. Nagaosa, and X. G. Wen, *Rev. Mod. Phys.* **78**, 17 (2006).  
<sup>5</sup> S. Sachdev, *Rev. Mod. Phys.* **75**, 913 (2003).  
<sup>6</sup> R. B. Laughlin, *Science* **242**, 525 (1988).  
<sup>7</sup> P. W. Anderson, *Science* **268**, 1154 (1995).  
<sup>8</sup> E. Demler, W. Hanke, and S.-C. Zhang, *Rev. Mod. Phys.* **76**, 909 (2004).  
<sup>9</sup> C. M. Varma, *Phys. Rev. Lett.* **83**, 3538 (1999).  
<sup>10</sup> C. M. Varma, *Phys. Rev. B* **73**, 155113 (2006).  
<sup>11</sup> M. Greiter and R. Thomale, *Phys. Rev. Lett.* **99**, 027005 (2007).  
<sup>12</sup> B. Fauqué, Y. Sidis, V. Hinkov, S. Pailhes, C. T. Lin, X. Chaud, and P. Bourges, *Phys. Rev. Lett.* **96**, 197001 (2006).  
<sup>13</sup> C. M. Varma, P. B. Littlewood, S. Schmitt-Rink, E. Abrahams, and A. E. Ruckenstein, *Phys. Rev. Lett.* **63**, 1996 (1989).  
<sup>14</sup> M. Gurvitch and A. T. Fiory, *Phys. Rev. Lett.* **59**, 1337 (1987).  
<sup>15</sup> H. Takagi, B. Batlogg, H. L. Kao, J. Kwo, R. J. Cava, J. J. Krajewski, and W. F. Peck, *Phys. Rev. Lett.* **69**, 2975 (1992).  
<sup>16</sup> Y. Dagan, M. M. Qazilbash, C. P. Hill, V. N. Kulkarni, and R. L. Greene, *Phys. Rev. Lett.* **92**, 167001 (2004).  
<sup>17</sup> J. L. Tallon and J. W. Loram, *Physica C* **349**, 53 (2001).  
<sup>18</sup> L. Alff, Y. Krockenberger, B. Welter, M. Schonecke, R. Gross, D. Manske, and M. Naito, *Nature* **422**, 698 (2003).  
<sup>19</sup> D. v. d. Marel, H. J. A. Molegraaf, J. Zaanen, Z. Nussinov, F. Carbone, A. Damascelli, H. Eisaki, M. Greven, P. H. Kes, and M. Li, *Nature* **425**, 271 (2003).  
<sup>20</sup> S. H. Naqib, J. R. Cooper, J. L. Tallon, R. S. Islam, and R. A. Chakalov, *Phys. Rev. B* **71**, 054502 (2005).  
<sup>21</sup> S. A. Kivelson, I. P. Bindloss, E. Fradkin, V. Oganesyan, J. M. Tranquada, A. Kapitulnik, and C. Howald, *Rev. Mod. Phys.* **75**, 1201 (2003).  
<sup>22</sup> S. Chakravarty, R. B. Laughlin, D. K. Morr, and C. Nayak, *Phys. Rev. B* **63**, 094503 (2001).  
<sup>23</sup> J. X. Li, C. Q. Wu, and D.-H. Lee, *Phys. Rev. B* **74**, 184515 (2006).  
<sup>24</sup> V. J. Emery, *Phys. Rev. Lett.* **58**, 2794 (1987).  
<sup>25</sup> F. C. Zhang and T. M. Rice, *Phys. Rev. B* **37**, 3759 (1988).  
<sup>26</sup> H. Eskes and G. A. Sawatzky, *Phys. Rev. Lett.* **61**, 1415 (1988).  
<sup>27</sup> M. S. Hybertsen, M. Schlüter, and N. E. Christensen, *Phys. Rev. B* **39**, 9028 (1989).  
<sup>28</sup> M. S. Hybertsen, E. B. Stechel, M. Schlüter, and D. R. Jennison, *Phys. Rev. B* **41**, 11068 (1990).  
<sup>29</sup> T. M. Rice, F. Mila, and F. C. Zhang, *Phil. Trans. R. Soc. Lond. A* **334**, 459 (1991).  
<sup>30</sup> V. I. Belinicher, A. L. Chernyshev, and V. A. Shubin, *Phys. Rev. B* **53**, 335 (1996).  
<sup>31</sup> S. Lee, J. B. Marston, and J. O. Fjærestad, *Phys. Rev. B* **72**, 075126 (2005).  
<sup>32</sup> J. O. Fjærestad, J. B. Marston, and U. Schollwöck, *Ann. Phys.* **321**, 894 (2005).  
<sup>33</sup> R. E. Walstedt and W. W. Warren, Jr., *Science* **248**, 1082 (1990).  
<sup>34</sup> L. H. Tjeng *et al.*, *Phys. Rev. Lett.* **78**, 1126 (1997).  
<sup>35</sup> A. Kaminski *et al.*, *Nature* **416**, 610 (2002).  
<sup>36</sup> S. V. Borisenko, A. A. Kordyuk, A. Koitzsch, T. K. Kim, K. A. Nenkov, M. Knupfer, J. Fink, C. Grazioli, S. Turchini, and H. Berger, *Phys. Rev. Lett.* **92**, 207001 (2004).  
<sup>37</sup> V. Aji and C. M. Varma, *Phys. Rev. Lett.* **99**, 067003 (2007).  
<sup>38</sup> E. Dagotto, *Rev. Mod. Phys.* **66**, 763 (1994).  
<sup>39</sup> S.-H. Lee *et al.*, *Phys. Rev. B* **60**, 10405 (1999).  
<sup>40</sup> S. Kremer, J. Brinckmann, and P. Wölfle, unpublished.